Available online at www.sciencedirect.com
SCIENCE DIRECT®
Energy Conversion and Management 46 (2005) 1083–1105
ENERGY CONVERSION & MANAGEMENT
www.elsevier.com/locate/enconman

Performance analysis of cascaded thermoelectric converters for advanced radioisotope power systems

Mohamed S. El-Genk *, Hamed H. Saber

Department of Chemical and Nuclear Engineering, Institute for Space and Nuclear Power Studies, The University of New Mexico, Albuquerque, NM 87131, USA

Received 10 March 2004; accepted 13 June 2004
Available online 1 September 2004

Abstract

Advanced radioisotope power systems (ARPSs) for future planetary missions require higher conversion efficiency than the state-of-the-art (SOA) SiGe thermoelectric converter in order to decrease system mass and reduce mission cost. The performance of three cascaded thermoelectric converters (CTCs) for potential use in ARPSs is investigated at heat rejection temperatures of 375, 475 and 575 K and input thermal powers of 1, 2 and 3 W_{th}. These CTCs have top SiGe unicouples that are thermally, but not electrically, coupled to bottom unicouples having one of the following compositions: (a) TAGS-85 (p-leg) and 2N–PbTe (n-leg); (b) $CeFe_{3.5}Co_{0.5}Sb_{12}$ (p-leg) and $CoSb_3$ (n-leg); and (c) segmented p-leg of $CeFe_{3.5}Co_{0.5}Sb_{12}$ and Zn_4Sb_3 and n-leg of $CoSb_3$. The top and bottom unicouples in the CTCs are of the same length (10 mm), but the optimized cross-sectional areas of the n- and p-legs for maximum efficiency are different. The nominal hot junction temperature of the top SiGe unicouples at their peak efficiencies is 1273 K and that of the cold junction is 780 K when the bottom unicouple is of composition (a) and 980 K for compositions (b) and (c). The hot junction temperatures of the bottom unicouples are taken 20 K lower than the cold junctions of the top unicouples, but the input thermal powers to the former are the same as those rejected by the latter. Assuming zero side heat losses and a contact resistance of 150 $\mu\Omega cm^2$ per leg in the top and bottom unicouples, the calculated peak efficiencies of the CTCs vary from 9.43% to 14.35%. These efficiencies are 40–113% higher, respectively, than that of SOA SiGe (~6.5%) when operating at the cold junction temperature of 566 K and the same hot junction temperature (1273 K) and contact resistance per leg. Decreasing this

* Corresponding author. Tel.: +1 505 277 5442; fax: +1 505 277 2814.
E-mail address: mgenk@unm.edu (M.S. El-Genk).

0196-8904/$ - see front matter
doi:10.1016/j.enconman.2004.06.019

resistance to a realistic value of 50 $\mu\Omega cm^2$ per leg increases the peak efficiencies of the CTCs by 0.5–0.9 percentage points to 9.93–15.25%.

Keywords: Cascaded thermoelectric converter (CTC); Skutterudites; Segmented thermoelectric; Energy conversion; SiGe; Advanced radioisotope power systems (ARPSs); Radioisotope thermoelectric generators (RTGs)

1. Introduction

Future exploration of the outer planets requires advanced nuclear power systems capable of providing electric power from a few Watts to hundreds of kilowatts for 7–10 years. For these planets, solar power is not an enabling option due to the progressively weaker solar brightness; on Mars, it is ~45% of that in earth orbit, <4% on Jupiter and essentially nil on other planets farther out. The solar option has been considered for a number of robotic and spacecraft missions to Mars. These missions typically have limited scope and duration from a few days to several months and require only a few to 10's of Watts of electrical power. For higher power missions to either Mars or the farthest planets, such as Jupiter, Saturn and Pluto, the solar option is not a viable one. Future exploration of these planets will require developing advanced energy conversion technologies that could be used with either a radioactive or a nuclear reactor heat source to provide a wide range of electrical power levels for 7–10 year missions, or even longer. These nuclear power systems operate continuously and independently of the sun.

Space reactor power systems (SRPSs) and advanced radioisotope power systems (ARPSs) each *enable* certain classes of missions. The SRPSs use fission nuclear reactors capable of generating hundred to thousands of kilowatts of thermal power continuously for 7–10 years. These reactors do not start until the spacecraft is fully and safely deployed into space. ARPSs use SOA general purpose heat source (GPHS) bricks that have been used in radioisotope thermoelectric generators (RTGs) on numerous planetary missions for more than three decades [1–3]. Each GPHS brick (or module) is loaded with four $^{238}PuO_2$ fuel pellets that each generates ~62.5 W of thermal power by the radioactive decay of the ^{238}Pu isotope. The relatively long half life (87 years) of ^{238}Pu makes it suitable for missions of 5 or more years with a small decrease in the thermal power to the end-of-mission (EOM). However, because of the low thermal power density of the $^{238}PuO_2$ fuel (~0.4 kW_{th}/kg) and its high density (>1000 kg/m^3), limited availability and high cost, ARPSs are only practical for those missions requiring a few tens to a thousand of Watts of electricity. Therefore, ARPSs are *enabling* deep space and long duration surface and limited subsurface exploration missions on Mars and the farthest planets in the solar system.

On the other hand, SRPSs are enabling high power interplanetary missions to propel large spacecraft using a multitude of high power electric propulsion engines requiring 100–250 kW_e, and even more. SRPSs markedly shorten the travel time to destination planets, significantly increase the delivered payload mass and provide ample electrical power for the science payload, fast communication and high data transmission rates, surface and subsurface operations and future space colonies. Unlike ARPSs, SRPSs could be designed to operate at variable power levels and for multiple shutdowns and restarts, as needed.

Nomenclature

A_n	cross-sectional area of n-type leg (m^2)
A_p	cross-sectional area of p-type leg (m^2)
k	thermal conductivity of thermoelectric materials ($W\,m^{-1}\,K^{-1}$)
$P_{e,CTC}$	nominal electric power of cascaded thermoelectric converter (W_e)
$Q_{in,CTC}$	input thermal power to top unicouple (W_{th})
r_{cont}	contact resistance per leg ($\mu\Omega\,cm^2$)
R_L	load resistance (Ω)
$T_{c,B}$	cold junction temperature of bottom unicouple (K)
$T_{c,T}$	cold junction temperature of top unicouple (K)
$T_{h,B}$	hot junction temperature of bottom unicouple (K)
$T_{h,T}$	hot junction temperature of top unicouple (K)
T_R	heat rejection temperature (K)
V_{oc}	open circuit voltage (V)
Z	thermoelectric material figure-of-merit, $\alpha^2/\rho k$ (K^{-1})

Greek symbols

α	Seebeck coefficient ($V\,K^{-1}$)
$\Delta T_{cj,R}$	difference between cold junction temperature of bottom unicouple and that of heat rejection ($T_{c,B} - T_R$)
Γ	ratio of cross-sectional areas of n- and p-legs of top and bottom unicouples (Eq. (2))
η_{CTC}	nominal peak efficiency of CTC (%)
η_B	conversion efficiency of bottom unicouple (%)
η_{SiGe}	conversion efficiency of top SiGe unicouple (%)
ρ	electrical resistivity of thermoelectric materials ($\Omega\,m$)

Subscripts

T	top unicouple
B	bottom unicouple

A key to enhancing the performance of both ARPSs and SRPSs and reducing their masses and mission costs is developing high efficiency, energy conversion technologies. For ARPSs, candidate technologies are those that could increase the conversion efficiency of the system by >50%, compared to SOA RTGs (~4.6%), and decrease the system's specific mass in kg/kW_e (or Alpha) by a similar percentage. It is worth noting that the projected Alpha for ARPSs (~100–200 kg/kW_e) is typically 4–5 times that for SRPSs, which explains why the latter are the preferred choice for high electrical power missions.

SOA RTGs use SiGe thermoelectric converters that operate typically at hot and cold junctions temperatures of 1273 and ~566 K, respectively. These converters have accumulated tens of years of remarkable performance on many missions to the sun and various planets in the solar system, such as Mars, Jupiter and Saturn [1–3]. SiGe thermoelectric converters have also been used, or

considered for use, in SRPSs with a system efficiency of up to 4.6% [4,5]. A SOA RTG typically generates $\simeq$290 W_e, however, its low efficiency (<5%) increases the amount of $^{238}PuO_2$ fuel needed. Earlier radioisotope space power systems had used lead telluride (PbTe) and silver antimony germanium telluride (TAGS-85) thermoelectric converters at hot and cold junction temperatures of ~785–800 and 450 K, respectively, and system efficiencies of ~6.2–6.4% [1,2,6].

The thermoelectric efficiency is directly proportional to the average figure of merit, Z of the thermoelectric materials in the n- and p-legs, where $Z = (\alpha^2/\rho k)$. As shown in Fig. 1, each thermoelectric material has high Z values only in a certain temperature range. Thus, in segmented thermoelectric converters (STCs) [7–14], the p- and n-legs each may be comprised of two or more segments of different but compatible TE materials, depending on the value of the cold junction temperature. The length of each segment is sized to operate in the temperature range in which the thermoelectric material has the highest Z value. The segments in the n- and p-legs are joined with minimal thermal and electrical interface resistances and no or minimal materials diffusion across the interfaces. STCs comprised of BiTe cold segments and Skutterudites [15,16] hot segments could be used in waste heat recovery in heavy trucks and a host of other terrestrial applications in which the hot junction temperature is 673–873 K and the cold junction temperature is 298 K. The conversion efficiencies of these STCs could be 13–15% and 10.9–13.3%, when assuming zero side heat losses and a contact resistance per leg of 150 $\mu\Omega cm^2$ and zero, respectively [8–10].

Skutterudites with high Z T from ~0.92 to 1.48 in the temperature range from 300 to 973 K have recently been developed at the Jet Propulsion Laboratory (JPL) in Pasadena, California, [15,16]. A number of STCs unicouples have been fabricated using p-type $CeFe_4CoSb_{12}$ and Bi_2Te_3-based alloys and n-type $CoSb_3$ based alloy and tested at cold and hot junction temperatures of 300 and 973 K, respectively [7,12,13]. Recent tests performed both at JPL and the University of New Mexico's Institute for Space and Nuclear Power Studies (UNM-ISNPS) demonstrated peak conversion efficiency for these STCs of 13.8%. However, since SiGe is not compatible with Skutterudites and because no other materials have yet been identified for operating at >973 K, CTCs could take advantage of the high temperature FOM of SiGe and the high FOM of Skutterudites for temperatures $\leqslant$ 973 K [14,17] (Fig. 1). The CTCs optimized to operate

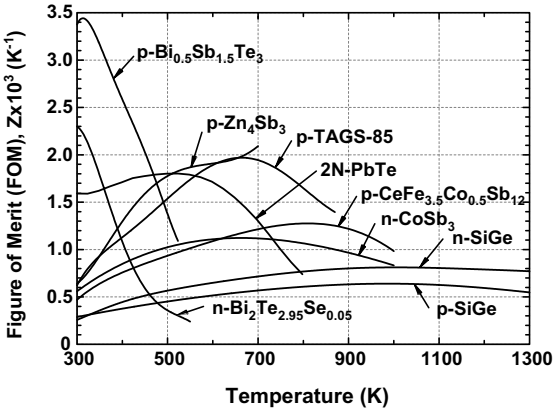

Fig. 1. FOMs of different thermoelectric materials.

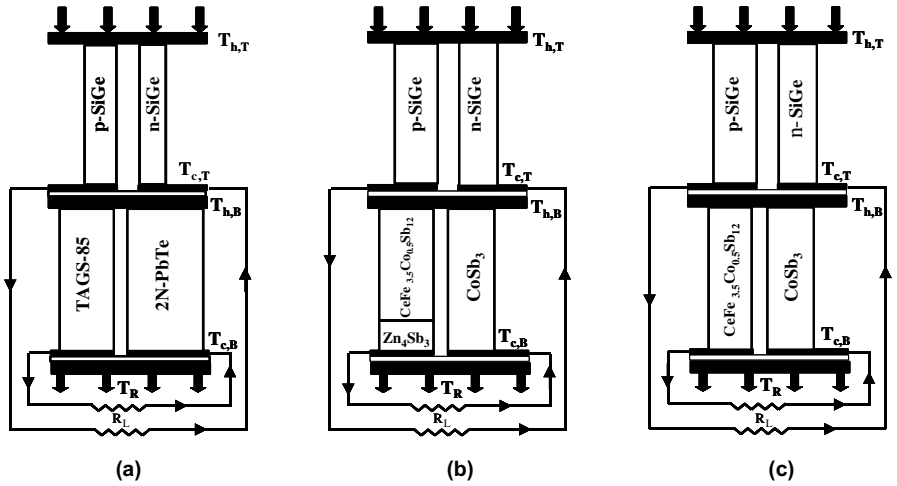

Fig. 2. Schematics of cascaded thermoelectric converters (CTCs). (a) CTC with TAGS-85/2N–PeTe bottom unicouple. (b) Segmented C with unicouple. (c) CTC with Skutterudites unicouple.

at hot junction temperatures up to 1273 K could have higher conversion efficiency than SOA SiGe, reducing the amount of $^{238}PuO_2$ fuel, the ARPS total mass and the mission cost [17].

This paper presents the performance results of three CTCs for use in ARPSs at significantly higher conversion efficiencies than that of SOA RTGs. The CTCs investigated are optimized for maximum efficiency operation. They have top SiGe unicouples and bottom unicouples with one of the following compositions (Figs. 1 and 2): (a) TAGS-85 (p-leg) and 2N–PbTe (n-leg); (b) p-leg of $CeFe_{3.5}Co_{0.5}Sb_{12}$ and n-leg of $CoSb_3$; and (c) segmented p-leg of $CeFe_{3.5}Co_{0.5}Sb_{12}$ and Zn_4Sb_3 and n-leg of $CoSb_3$. The performance analyses of the CTCs are conducted for a nominal hot junction temperature for the SiGe top unicouples of 1273 K, three input thermal power values, $Q_{in,CTC}$, of 1, 2 and 3 W_{th} and three heat rejection temperatures, T_R, from the bottom unicouples of 375, 475 and 575 K. The values of $Q_{in,CTC}$ cover a wide range of heat fluxes in the n- and p-legs that are inclusive of potential integration into either ARPSs or SRPSs. The top and bottom unicouples in the CTCs (Figs. 2(a)–(c)) are thermally, but not electrically, coupled. Also, the rates of heat rejection from the top SiGe unicouples are the same as the rates of heat input to the bottom unicouples. The analyses assume zero side heat losses and a contact resistance of 150 $\mu\Omega cm^2$ per leg in both the top and bottom unicouples; however, the effect of reducing this resistance to a more realistic value of 50 $\mu\Omega cm^2$ per leg on the performance of the CTCs is investigated.

2. Cascaded thermoelectric converters

The three CTCs analyzed in this paper are depicted in Figs. 2(a)–(c). The total lengths of the top and bottom uncouples are the same (10 mm), however, the optimized cross-section areas of the n- and p-legs for each unicouple are different. The effective hot junction temperature of the top SiGe unicouples, $T_{h,T}$, varies with the load current, but its nominal value at the peak efficiency is 1273 K. The cold junction temperature of the SiGe unicouple in the CTC in Fig. 2(a) is kept

constant at 780 K and at 980 K for the CTCs in Figs. 2(b) and (c). These temperatures are used in the optimization of the cross-section areas of the n- and p-legs of the SiGe unicouples for maximum efficiency operation. The cross-section areas of the legs for the bottom unicouples are also optimized for maximum efficiency at nominal cold junction temperatures, $T_{c,B}$, that are 25 K higher than T_R and hot junction temperatures that are 20 K lower than those of the cold junctions of the top SiGe unicouples.

The determination of the optimum cross-sectional areas of the n- and p-legs in the top and bottom unicouples for specified input thermal power, $Q_{in,CTC}$, and hot and cold junctions temperatures is done using a 1-D design and optimization model of segmented and non-segmented thermoelectric unicouples [8,11]. The optimization analyses assumes zero side heat losses from the top and bottom unicouples in the CTCs, which is reasonable since, in actual space nuclear power systems, the n- and p-legs will be well insulated. The analyses account for the change in the properties of the thermoelectric materials in the n- and p-legs with temperature and conservatively assume a contact resistance of 150 $\mu\Omega cm^2$ per leg in the top and bottom unicouples. The effect of decreasing this resistance to a more realistic value of 50 $\mu\Omega cm^2$ per leg on the performance of the CTCs is investigated.

2.1. Optimization CTCs efficiency

The thermoelectric model used in the present analyses is coupled to a genetic algorithm for determining the cross-section areas of the n- and p-legs for either maximum efficiency or maximum electrical power density operation [8,11]. The optimization of the CTCs in Figs. 2(a)–(c) is carried out in two successive steps. First, the cross sectional areas of the n- and p-legs of the top SiGe unicouple are optimized for maximum efficiency operation at a nominal hot junction temperature of 1273 K, constant cold junction temperature of either 780 K (Fig. 2(a)) or 980 K (Figs. 2(b) and (c)) and input thermal power of either 1.0, 2.0 or 3.0 W_{th}. The calculated heat rejected rate from the top SiGe unicouples is taken the same as the input thermal power to the bottom unicouple ($Q_{in,CTC}$ $(1-\eta_{SiGe})$). Then the cross-sectional areas of the n- and p-legs of the bottom unicouples (Figs. 2(a)–(c)) are optimized for maximum efficiency operation at constant cold junction temperatures that are 25 K higher than the specified heat rejection temperature, T_R, of 375, 475 or 575 K.

2.2. Calculation of CTCs efficiency

The nominal peak efficiency of the CTCs, η_{CTC}, that corresponds to the peak efficiency of the top SiGe unicouple, η_{SiGe}, is expressed as

$$\eta_{CTC} = \eta_{SiGe} + (1-\eta_{SiGe})\eta_B. \quad (1)$$

In this equation, η_B is the nominal conversion efficiency of the bottom unicouple. The nominal voltages at η_{CTC} are different for the top and bottom unicouples, however, in actual ARPSs, the top and bottom unicouples will be assembled into arrays, each of which is made up of a multitude of unicouples that are connected electrically in series. The number of unicouples in the top and bottom arrays would be selected such that the arrays operate at the same nominal voltage but not necessarily the same load current [17]. Because of the difference in the thermoelectric

properties, the number and the cross section areas of the legs in the SiGe unicouples in the top array will be different than those for the unicouples in the bottom array [17]. The next section presents and compares the performance of the CTCs in Figs. 2(a)–(c) and the contributions of the top and bottom unicouples.

3. Results

In this section, the performance results assuming a total contact resistance of 150 $\mu\Omega cm^2$ per leg in both the top and bottom unicouples of the CTCs in Fig. 2 are presented and compared with those using a more realistic resistance of 50 $\mu\Omega cm^2$ per leg. The performance results of the CTCs, assuming a contact resistance of 150 $\mu\Omega cm^2$ per leg, are also listed in Tables 1 and 2. The results of the effects of changing the input thermal power, $Q_{in,CTC}$, to the top SiGe unicouples (1.0, 2.0 and 3.0 W_{th}) and the heat rejection temperature, T_R, from the bottom unicouples (375, 475 and 575 K) on the performance parameters of the CTCs are also presented and discussed. These parameters include the nominal peak efficiencies and corresponding electric powers, the nominal terminal voltages and the ratios of the optimized cross-sectional areas of the n- and p-legs of the top and bottom unicouples.

3.1. Performance of SiGe top stage unicouples

The nominal efficiencies and electric powers of the top SiGe unicouples in the CTCs in Fig. 2 depend on the values of $Q_{in,CTC}$ and $T_{c,T}$. As indicated earlier, $T_{c,T}$ is taken = 780 K for the CTC in Fig. 2(a) and 980 K for the CTCs in Figs. 2(b) and (c). These cold junction temperatures and, hence, the hot junction temperatures of the bottom unicouples, $T_{h,B}$, are based on those recommended for the thermoelectric materials used in the bottom unicouples (Fig. 1). To avoid excessive sublimation of the PbTe and TAGS-85 of the bottom unicouple in Fig. 2(a), the hot junction temperature, $T_{h,B}$, is kept below 773 K (or 500 °C). Similarly, for long operation time of the Skutterudites ($CeFe_{3.5}Co_{0.5}Sb_{12}$ and $CoSb_3$) used in the bottom unicouples in Figs. 2(b) and (c), $T_{h,B}$ is kept below 973 K (or 700 °C).

The results delineated in Fig. 3 show the effect of the input thermal power, $Q_{in,CTC}$, on the voltage–current (V–I) characteristics, efficiency and electrical power of the top SiGe unicouples. Fig. 3(a) indicates that the open circuit voltage (at zero current), V_{oc}, is independent of $Q_{in,CTC}$ but depends on the value of the cold junction temperature, $T_{c,T}$. When this temperature is 780 K (Fig. 2(a)), V_{oc} = 0.333 V and decreases to 0.203 V when this temperature is 980 K (Figs. 2(b) and (c)). Conversely, Figs. 3(b) and (c) show that at the same $Q_{in,\ CTC}$, the lower $T_{c,T}$ increases the nominal peak conversion efficiencies and the corresponding electrical powers of the top SiGe unicouples (Fig. 3 and Table 1). The nominal electrical powers of the top SiGe unicouples increase linearly with increasing $Q_{in,CTC}$ (Fig. 3(c)).

The peak efficiencies of the SiGe unicouples in the CTCs with the configurations in Figs. 2 are the same (3.44%), but much lower than that for the SiGe unicouple of the CTC in Fig. 2(a) (5.87%) because of the lower cold junction temperature of the latter ($T_{c,T}$ = 780 K). However, the higher average FOM of the materials (Fig. 1) and the corresponding higher hot junction temperature of the bottom unicouples (960 K) of the CTCs in Figs. 2(b) and (c) more than

Table 1
Summary of design optimization and performance parameters of CTCs in Figs. 2(a)–(c)

Parameter	Cascaded thermoelectric converter (CTC)														
	Top (Fig. 2(a))			Bottom (Fig. 2(a))			Top (Figs. 2(b) and (c))			Bottom (Fig. 2(b))			Bottom (Fig. 2(c))		
$Q_{in,CTC}$ (W_{th})	1.0	2.0	3.0	0.94	1.88	2.82	1.0	2.0	3.0	0.97	1.93	2.90	0.97	1.93	2.90
Rejection temperature of 375 K															
p-leg (mm^2)	1.73	3.45	5.18	4.90	9.80	14.7	2.85	5.69	8.54	3.48	6.97	10.5	2.24	4.48	6.72
n-leg (mm^2)	1.73	3.45	5.18	8.12	16.2	24.4	2.85	5.69	8.54	2.33	4.67	7.00	2.34	4. 68	7.02
Rejection (W_{th})	0.94	1.88	2.82	0.86	1.72	2.58	0.97	1.93	2.90	0.86	1.71	2.57	0.87	1.74	2.61
Current (A)	0.36	0.73	1.09	0.86	1.71	2.56	0.34	0.68	1.02	0.88	1.76	2.64	8.32	1.66	2.49
Efficiency (%)	5.87	5.87	5.87	8.77	8.77	8.77	3.44	3.44	3.44	11.3	11.3	11.3	9.93	9.93	9.93
Electric power (mW_e)	58.7	117	176	82.5	165	248	34.4	68.8	103	109	218	326	95.9	192	288
Voltage (mV)	161	161	161	96.5	96.5	96.5	101	101	101	124	124	124	115	115	115
Specific power (W_e/kg)	569	569	569	84	84	84	202	202	202	246	246	246	271	271	271
Power density (W_e/cm^3)	1.70	1.70	1.70	0.63	0.63	0.63	0.60	0.60	0.60	1.87	1.87	1.87	2.09	2.09	2.09
Input heat flux (W_{th}/cm^2)	29.0	29.0	29.0	7.2	7.2	7.2	17.6	17.6	17.6	16.6	16.6	16.6	21.1	21.1	21.1
p-leg hot and cold segments (mm)	–	–	–	–	–	–	–	–	–	8.02 1.98	8.02 1.98	8.02 1.98	–	–	–
Rejection temperature of 475 K															
p-leg (mm^2)	1.73	3.45	5.18	6.59	13.2	19.8	2.85	5.69	8.54	3.80	7.60	11.4	2.73	5.46	8.19
n-leg (mm^2)	1.73	3.45	5.18	12.4	24.8	37.2	2.85	5.69	8.54	2.87	5.74	8.6	2.86	5.73	8.59
Rejection (W_{th})	0.94	1.88	2.82	0.88	1.75	2.64	0.97	1.93	2.90	0.88	1.75	2.63	0.89	1.77	2.65
Current (A)	0.36	0.73	1.09	0.80	1.60	2.41	0.34	0.68	1.02	0.82	1.65	2.47	0.80	1.59	2.39
Efficiency (%)	5.87	5.87	5.87	6.42	6.42	6.42	3.44	3.44	3.44	9.24	9.24	9.24	8.39	8.39	8.39
Electric power (mW_e)	58.7	117	176	60.5	121	181	34.4	68.8	103	89.2	178	268	81.0	162	243
Voltage (mV)	161	161	161	75.3	75.3	75.3	101	101	101	108	108	108	102	102	102
Specific power (W_e/kg)	569	569	569	42	42	42	202	202	202	175	175	175	187	187	187
Power density (W_e/cm^3)	1.70	1.70	1.70	0.32	0.32	0.32	0.60	0.60	0.60	1.34	1.34	1.34	1.45	1.45	1.45
Input heat flux (W_{th}/cm^2)	29.0	29.0	29.0	5.0	5.0	5.0	17.6	17.6	17.6	14.5	14.5	14.5	17.3	17.3	17.3
p-leg hot and cold segments (mm)	–	–	–	–	–	–	–	–	–	8.62 1.38	8.62 1.38	8.62 1.38	–	–	–
Rejection temperature of 575 K															
p-leg (mm^2)	1.73	3.45	5.18	10.4	20.9	31.3	2.85	5.69	8.54	4.16	8.33	12.5	3.48	6.97	10.5
n-leg (mm^2)	1.73	3.45	5.18	21.7	43.3	65	2.85	5.69	8.54	3.63	7.27	10.9	3.63	7.26	10.9

Rejection (W_{th})	0.94	1.88	2.82	0.91	1.81	2.72	0.97	1.93	2.90	0.90	1.80	2.70	0.90	1.80	2.90
Current (A)	0.36	0.73	1.09	0.72	1.44	2.15	0.34	0.68	1.02	0.77	1.54	2.31	0.76	1.52	2.28
Efficiency (%)	5.87	5.87	5.87	3.78	3.78	3.78	3.44	3.44	3.44	6.93	6.93	6.93	6.57	6.57	6.57
Electric power (mW_e)	58.7	117	176	35.6	71.2	107	34.4	68.8	103	66.9	134	201	63.4	127	190
Voltage (mV)	161	161	161	49.6	49.6	49.6	101	101	101	86.8	86.8	86.8	83.6	83.6	83.6
Specific power (W_e/kg)	569	569	569	15	15	15	202	202	202	112	112	112	115	115	115
Power density (W_e/cm^3)	1.70	1.70	1.70	0.11	0.11	0.11	0.60	0.60	0.60	0.86	0.86	0.86	0.89	0.89	0.89
Input heat flux (W_{th}/cm^2)	29.0	29.0	29.0	2.9	2.9	2.9	17.6	17.6	17.6	12.4	12.4	12.4	13.6	13.6	13.6
p-leg hot and cold segments (mm)	–	–	–	–	–	–	–	–	–	9.3 0.7	9.3 0.7	9.3 0.7	–	–	–

Table 2
CTCs performance summary

Parameter	CTC in Fig. 2(a)			CTC in Fig. 2(b)			CTC in Fig. 2(c)		
$T_R = 375$ K									
$Q_{in,CTC}$ (W_{th})	1.0	2.0	3.0	1.0	2.0	3.0	1.0	2.0	3.0
η_{CTC} (%)		14.13			14.35			13.03	
$P_{e,CTC}$ (mW_e)	141.2	282	424	143.4	286.8	429	130.3	260.8	391
$T_R = 475$ K									
η_{CTC} (%)		11.91			12.36			11.54	
$P_{e,CTC}$ (mW_e)	119.2	238	357	123.6	246.8	371	115.4	230.8	346
$T_R = 575$ K									
η_{CTC} (%)		9.43			10.13			9.78	
$P_{e,CTC}$ (mW_e)	94.3	188.2	283	101.3	202.8	304	97.8	195.8	293

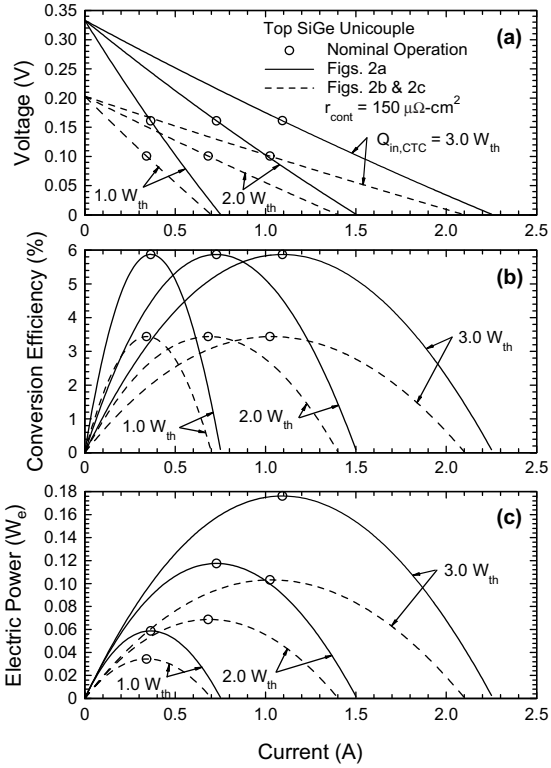

Fig. 3. Performance results of top SiGe unicouples.

compensate for the lower nominal efficiency of the top SiGe unicouples, resulting in higher efficiencies for the CTCs (Table 2). This and Table 1 and Figs. 4 and 5 show that increasing the heat rejection temperature, T_R, decreases the conversion efficiencies of the bottom unicouples and

those of the CTCs. On the other hand, increasing $Q_{in,CTC}$ does not change the nominal peak efficiencies of the top SiGe unicouples but shifts them to higher currents and, hence, higher electric powers (Figs. 3–5). The electrical power generated by the SiGe unicouple of the CTC in Fig. 2(a) increases from 0.059 to 0.176 W_e as $Q_{in,CTC}$ increases from 1.0 to 3.0 W_{th}, respectively. The corresponding nominal electric powers generated by the top SiGe unicouples of the CTCs in Figs. 2(b) and (c) are lower; they are 0.034 and 0.109 W_e, respectively.

Additional performance parameters that depend on the total size and mass of the optimized top and bottom unicouples in the CTCs are the specific powers and power densities of the thermoelectric materials of these unicouples. These values are 569 W_e/kg and 1.7 W_e/cm^2, respectively, for the top SiGe unicouple of the CTC in Fig. 2(a) and significantly lower at 202 W_e/kg and 0.6 W_e/cm^2, respectively, for the CTCs in Figs. 2(b) and (c) (Table 1). The indicated values for the SiGe unicouples are independent of $Q_{in,\ CTC}$ and T_R but depend on $T_{C,T}$, and those of the bottom unicouples are independent of $Q_{in,CTC}$ but depend on the type of thermoelectric materials, $T_{C,T}$ and T_R. When T_R = 375 K, the specific power and power density of the bottom unicouple of the CTC in Fig. 2(a) are only 84 W_e/kg and 0.63 W_e/cm^2 and decrease to 15 W_e/kg and 0.11 W_e/cm^2, respectively, as T_R increases to 575 K (Table 1). Such low values are because the densities of the thermoelectric materials in the bottom unicouple of the CTC in Fig. 2(a) (2N–PbTe for the n-leg and TAGS-85 for the p-leg) are much higher than that of SiGe. When the bottom unicouples

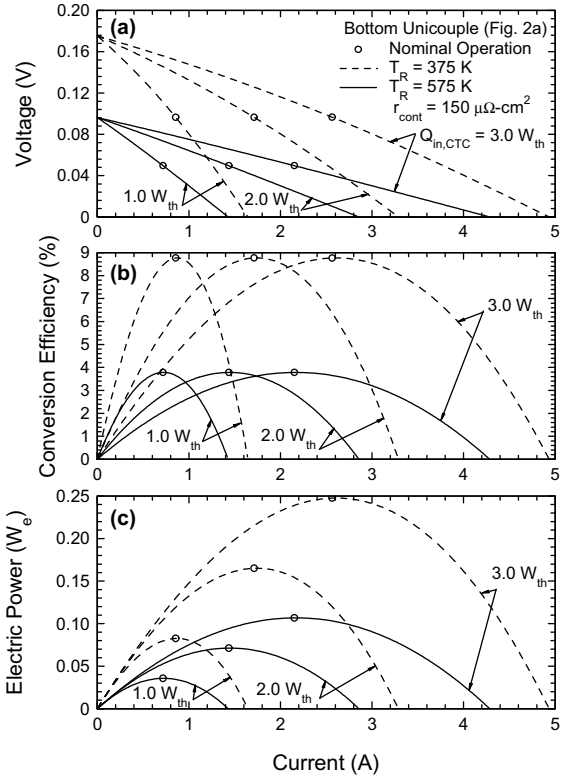

Fig. 4. Performance results of bottom unicouple in CTC in Fig. 2(a).

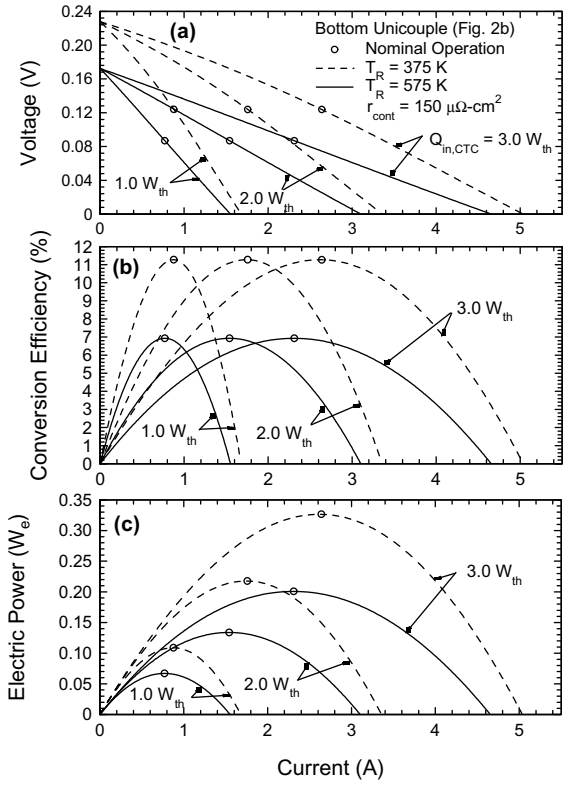

Fig. 5. Performance results of bottom unicouple in CTC in Fig. 2(b).

are made of Skutterudites (Figs. 2(b) and (c)); their specific powers and power densities also decrease with increasing T_R; they are much higher than those of the 2N–PeTe / TAGS-85 but lower than those of SiGe (Table 1).

3.2. Performance of bottom unicouples

As indicated earlier, the performance of the top SiGe unicouples is independent of T_R but depends on $T_{c,T}$. Figs. 4–6 present the performance results depicting the effects of $Q_{in,CTC}$, T_R and the type of thermoelectric materials on the performance of the bottom unicouples in the CTCs (Figs. 2(a)–(c)). Increasing T_R decreases the nominal efficiencies, the electrical powers and the open circuit voltages of the bottom unicouples (Figs. 4(a), 5(a) and 6(a)). While both the open circuit voltage and that at the peak conversion efficiency are independent of $Q_{in,CTC}$, the current at the peak efficiency increases with increasing $Q_{in,CTC}$ and/or decreasing T_R. The nominal efficiencies of the bottom unicouples (Figs. 4(b), 5(b) and 6(b)), which are also independent of $Q_{in,CTC}$, are much higher than those of the top SiGe unicouples (Fig. 3(b)). Theses efficiencies increase from 6.93% to 11.27% as T_R decreases from 575 to 375 K (Fig. 5(b)), or $T_{c,B}$ decreases from 600 to 400 K, respectively. When T_R = 375 K, the current at the peak efficiency of the bottom unicouple of the CTC in Fig. 2(b) increases from 0.88 to 2.64 A as $Q_{in,CTC}$ increases from 1.0 to 3.0

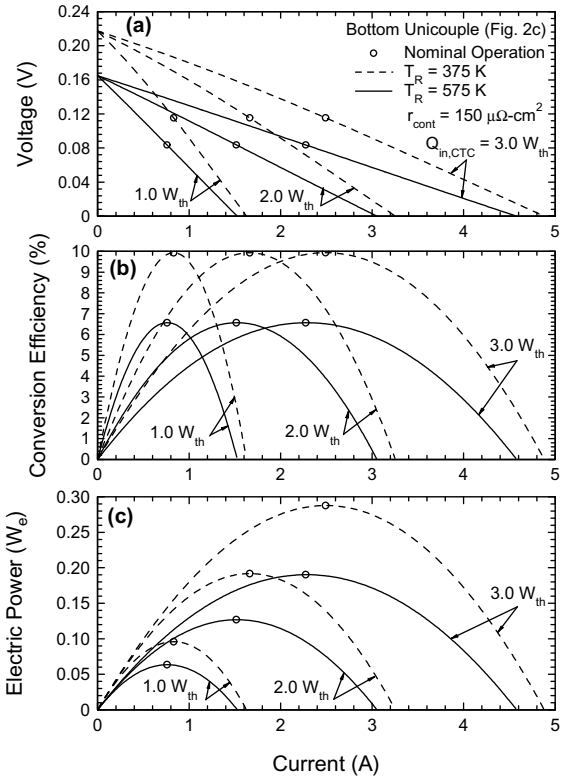

Fig. 6. Performance results of bottom unicouple in CTC in Fig. 2(c).

W_{th} (Fig. 5(b)). At the higher T_R of 575 K, this current is slightly lower, increasing from 0.77 to 2.31 A as $Q_{in,CTC}$ increases from 1.0 to 3.0 W_{th}. These currents are higher, but the corresponding voltages for the bottom unicouple of the CTC in Fig. 2(b) (Fig. 5(a)) are lower than those of the SiGe unicouple (Fig. 3(a)). The net effect is that the peak electrical powers of the bottom unicouples of the CTCs in Figs. 2(a) and (b) are higher than those for the top SiGe unicouples and increase with increasing $Q_{in,\ CTC}$ or decreasing T_R (Figs. 4–6).

For example, when $Q_{in,CTC}$ = 3.0 W_{th} the peak electrical power for the SiGe unicouple of the CTC shown in Fig. 2(b) is 0.103 W_e and independent of T_R (Fig. 3(c)). The peak electrical power of the bottom unicouple of the CTC in Fig. 2(b) increases from 0.20 to 0.33 W_e as T_R decreases from 575 to 375 K (Fig. 5(c)). Similar results are shown in Figs. 4(c) and 6(c) for the bottom unicouples of the CTCs in Figs. 2(a) and (c), respectively. Figs. 5(b) and 6(b) indicate that the segmented and Skutterudite based bottom unicouples of the CTCs in Figs. 2(b) and (c) operate at much higher nominal peak efficiencies than the 2N–PbTe/TAGS-85 bottom unicouple of the CTC in Fig. 2(a) (Fig. 4(b)). When T_R = 575 K, the nominal peak efficiency of the segmented bottom unicouple of the CTC in Fig. 2(b) is 6.93% and independent of $Q_{in,CTC}$; it increases to 11.3% as T_R decrease to 373 K (Fig. 5(b)). The second highest efficiency is that of the Skutterudites bottom unicouple of the CTC in Fig. 2(c) (Fig. 5(b)). The 2N–PbTe/TAGS-85 unicouple of the CTC in Fig. 2(a) has the lowest nominal efficiency that increases from 3.78% to 8.77% as T_R decreases

from 575 to 375 K (Fig. 4(b)). Such low efficiencies are mostly because the hot junction temperature of 760 K is much lower than those for the segmented and Skutterudites bottom unicouples of the CTCs in Figs. 2(b) and (c) (960 K). The FOM of the thermoelectric materials of the bottom unicouples in the respective CTCs (Fig. 1) also affects their nominal efficiencies and those of the CTCs (Tables 1 and 2).

3.3. Nominal efficiencies of CTCs

Fig. 7 compares the nominal efficiencies and electric powers of the optimized CTCs in Figs. 2(a)–(c), at different heat rejection temperatures, T_R. As indicated earlier, these efficiencies (Eq. (1)) are independent of $Q_{in,CTC}$ but strongly depend on the properties of the thermoelectric materials of the bottom unicouples and T_R. When T_R = 375 K, the nominal peak efficiency of the CTC in Fig. 2(a) is as high as 14.1% and decreases to 11.9% and 9.4% as T_R increases to 475 and 575 K, respectively (Fig. 7(a) and Table 2). It is worth noting that the nominal peak efficiency of the CTC in Fig. 2(a) is always higher than that of the CTC in Fig. 2(c), except when $T_R > 525$ K. When $T_R < 525$ K, the contribution of the thermoelectric materials in the bottom unicouple of the CTC in Fig. 2(a) more than makes up for the low hot junction temperature of the bottom unicouple (760 K). In addition, this low cold junction temperature (780 K) results in higher efficiency for the top SiGe unicouple. At higher T_R, however, the nominal efficiency of the CTC in Fig. 2(a) drops below that of the CTC in Fig. 2(c). The bottom unicouple of the CTC in Fig. 2(c) is made of Skutterudites (p-leg of $CeFe_{3.5}Co_{0.5}Sb_{12}$ and n-leg of $CoSb_3$). The high FOMs of these materials result in high efficiency for the bottom unicouple of the CTC in Fig. 2(c) when $T_R > 525$ K.

The results in Fig. 7(a) show that when $T_R < 525$ K, the CTC in Fig. 2(a) would be preferable to that in Fig. 2(c), while the latter would be preferable at higher T_R. For example, at T_R = 600 K, the peak nominal conversion efficiency of the CTC in Fig. 2(a) drops below 9%, while that of the CTC in Fig. 2(c) is slightly higher at ~9.3%. Fig. 7(a) also shows that the CTC in Fig. 2(b) is by

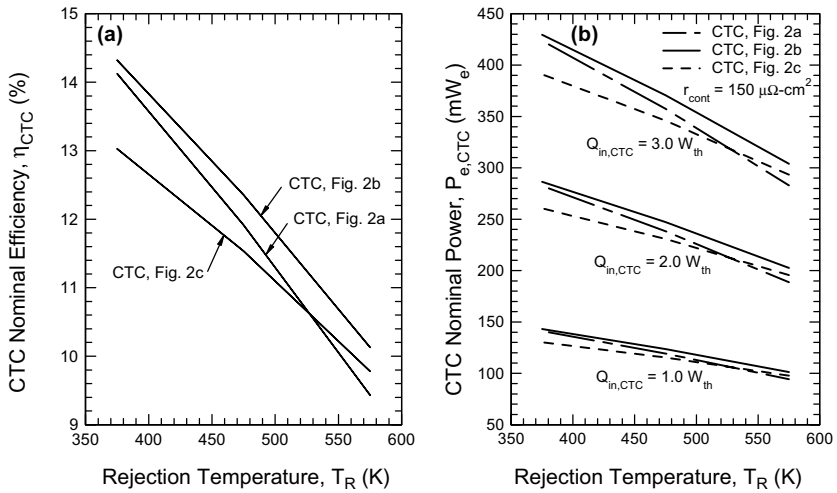

Fig. 7. Effect of rejection temperature on CTCs nominal efficiencies and electric powers.

far the best at all values of T_R. It has the highest nominal peak efficiencies; 14.35% at T_R = 375 K and 10.13% at T_R = 575 K (Table 2). The bottom unicouple of this CTC operates at the same hot junction temperature (960 K) as the one of the CTC in Fig. 2(c); but the p-leg is comprised of two segments: $CeFe_{3.5}Co_{0.5}Sb_{12}$ and Zn_4Sb_3 (Fig. 1). In this CTC (Fig. 2(b)), the nominal peak efficiency of the bottom unicouple decreases from 11.3% to 6.93% as T_R increases from 375 to 575 K. The corresponding values of the bottom unicouple of the CTC in Fig. 2(c) are 9.93% and 6.57%, respectively (Table 1 and Figs. 5(b) and 6(b)).

3.4. Nominal performance of CTCs

Fig. 7(b) and Table 2 compare the nominal electric powers of the CTCs in Figs. 2(a) and (c) as functions of T_R. The results that are consistent with those in Figs. 4(c), 5(c) and 6(c) show that the CTC in Fig. 2(b) generates the highest electrical powers. However, the differences in the values of the nominal electric powers of the CTCs in Fig. 2 decrease as $Q_{in,CTC}$ decreases (Fig. 7(b)). When T_R = 373 K, the highest nominal electrical power is generated by the CTC in Fig. 2(b); it is 429 mW_e when $Q_{in,CTC}$ = 3.0 W_{th} and decreases linearly to 143.4 mW_e as $Q_{in,CTC}$ decreases to 1.0 W_{th} (Table 2). These values of the nominal electric power decrease to 304 and 101.3 W_e, respectively, when T_R increases to 575 K. For the CTCs in Fig. 2, the cross-sectional areas of the n- and p-legs of the top and bottom unicouples that are optimized for maximum efficiency operation increase with increasing $Q_{in,CTC}$ at specified hot and cold junction temperatures (Table 1). The nominal efficiencies and voltages of the top and bottom unicouples are independent of $Q_{in,CTC}$ (Fig. 8(b)), but the nominal currents and electric powers increase with $Q_{in,CTC}$. The increases in the electric currents for the bottom unicouples with increasing $Q_{in,CTC}$ decrease slightly with increasing T_R, but those of the top unicouples are independent of T_R (Fig. 8(a)). The nominal current of the bottom unicouple of the CTC Fig. 2(b) is the highest, followed by that of the CTCs in Figs. 2(a) and (c), respectively. Fig. 8(a) shows that for the bottom unicouple of the CTC in Fig. 2(b),

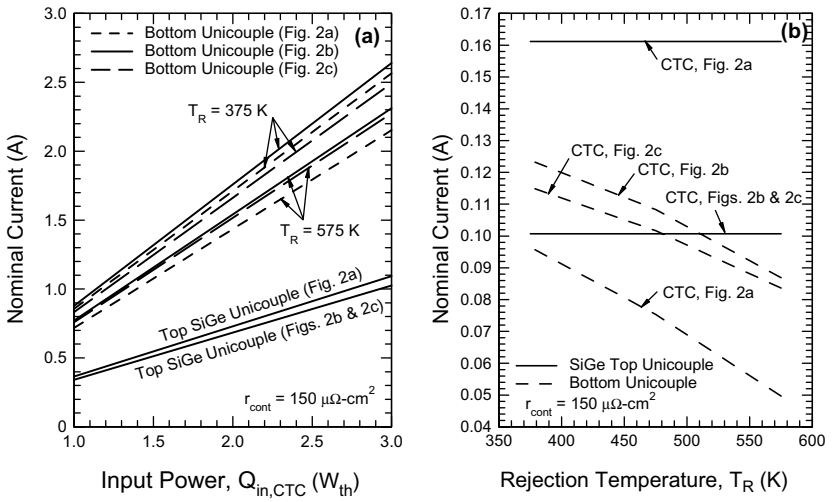

Fig. 8. Effects of input thermal power and rejection temperature on nominal currents and voltages of CTCs.

when T_R = 375 K, the nominal current increases linearly from 0.88 to 2.64 A as $Q_{in,\ CTC}$ increases from 1.0 to 3.0 W_{th}, while at T_R = 575 K, this current increases from 0.77 to 2.31 A, respectively.

Fig. 8(b) shows that the nominal voltage of the bottom unicouple of the CTC in Fig. 2(b) is the highest, followed by that of the CTC in Fig. 2(c), then the CTC in Fig. 2(a). These voltages decrease with increasing T_R. The nominal voltages of the top SiGe unicouples are independent of T_R but not those of the bottom unicouples in the CTCs in Fig. 2. The nominal voltage of the top SiGe unicouple is independent of T_R; it is much higher in the CTC in Fig. 2(a) because the cold junction temperature ($T_{c,T}$ = 780 K) is much lower than that of the CTCs in Figs. 2(b) and (c) ($T_{c,T}$ = 980 K). The nominal voltages of the top SiGe unicouples are 0.16 and 0.10 V when the cold junction temperature is 780 and 980 K, respectively (Figs. 2 and 8(b) and Table 1). For the bottom unicouples, the nominal voltage is independent of $Q_{in,CTC}$ but decreases linearly with increasing T_R. For the CTC in Fig. 2(b), the nominal voltage of the bottom segmented unicouple decreases from 0.124 to 0.09 V as T_R increases from 375 to 575 K. Table 1 lists the calculated values of the optimized cross sectional areas of the n- and p-legs and the nominal input heat fluxes for the top and bottom unicouples at different values of $Q_{in,CTC}$ and T_R.

3.5. Relative contributions of the top and bottom unicouples

Fig. 9 compares the relative contributions of the top and bottom unicouples to the nominal electrical powers and peak efficiencies of the CTCs in Figs. 2(a)–(c). The percentage contributions of the top and of the bottom unicouples to the nominal efficiencies and electrical powers of the CTCs are numerically the same, independent of $Q_{in,CTC}$ but change with T_R. Increasing T_R is shown earlier to decrease the nominal electric powers of the bottom unicouples but not those of the top SiGe unicouples. Therefore, the percentage contributions of the bottom unicouples decrease while those of the top SiGe unicouples increase as T_R increases (Fig. 9). When T_R = 375 K, the contributions of the bottom unicouple of the CTC in Fig. 2(b) of 76% are the highest; they decrease to 66% as T_R increases to 575 K. For the same increase in T_R, the contributions of the top SiGe unicouple in the same CTC increase from 24% to 34%, respectively. As delineated

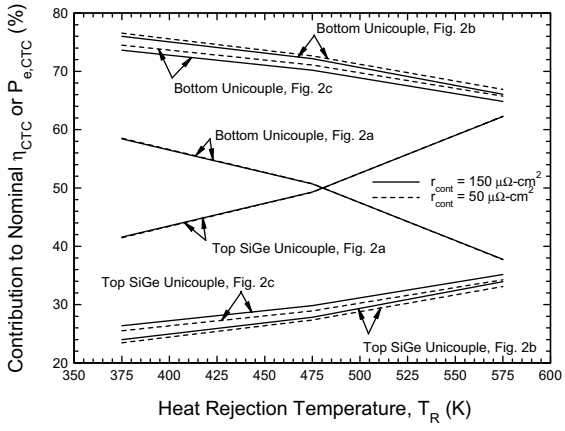

Fig. 9. Relative contributions of top and bottom unicouples.

in Fig. 9, the contributions of the top SiGe unicouple of the CTC in Fig. 2(b) is lowest, followed by those for the SiGe unicouple of the CTC in Fig. 2(c) and are highest for that of the CTC in Fig. 2(a). This is because, in the latter, the cold junction temperature of the top SiGe unicouple (780 K) is much lower than that (980 K) for the SiGe unicouples of the CTCs in Figs. 2(b) and (c).

3.6. Effect of contact resistance

In this section, the effects of decreasing the contract resistance from the assumed value in the analyses of 150 $\mu\Omega cm^2$ per leg in the top and bottom unicouples of the CTCs in Fig. 2 to a more realistic value of 50 $\mu\Omega cm^2$ per leg are investigated. Fig. 10 presents the results for the top SiGe unicouple of the CTC in Fig. 2(a), which indicate that decreasing the contact resistance slightly increases the peak conversion efficiency and the corresponding electric power and shifts them slightly to higher electric current. Similar results are obtained for the bottom unicouples. Figs. 11(a) and (b) show that reducing the contact resistance per leg in both the top and bottom unicouples increases the nominal efficiencies and electrical powers of the CTCs in Fig. 2. As shown in Figs. 11(a) and (b), the smallest increases in the nominal peak efficiency and electrical power are those of the CTC in Fig. 2(a); they range from ~0.3 to 0.5 percentage point or 3.2% to 3.54%, as the T_R decreases from 575 to 375 K, respectively. The largest increases in the nominal peak efficiency and electrical power are those of the CTC in Fig. 2(c); they range from 0.57 to 0.89

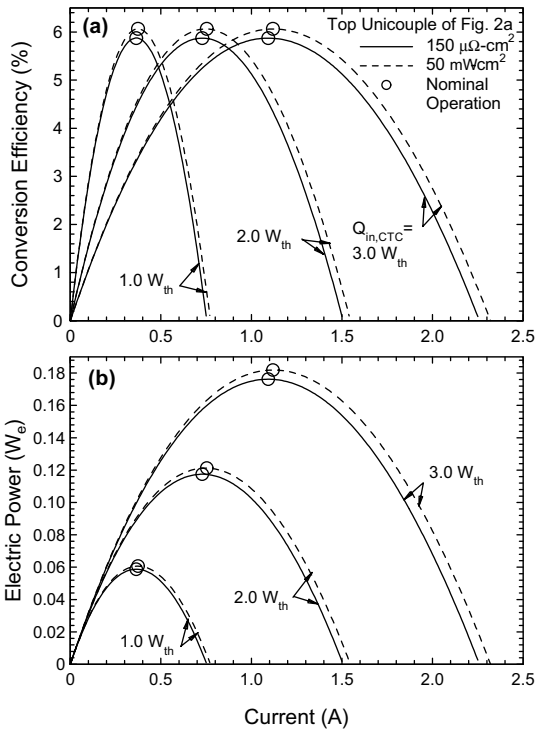

Fig. 10. Effect of contact resistance on performance for SiGe unicouple of CTC in Fig. 2(a).

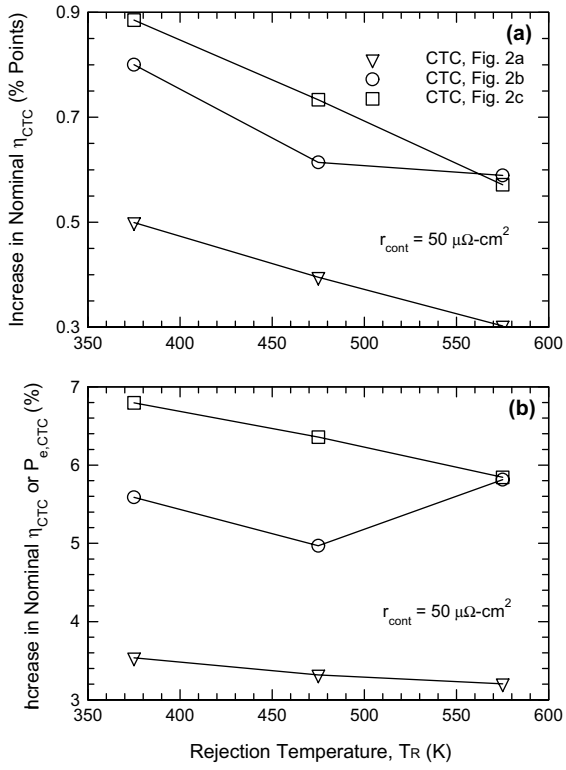

Fig. 11. Effect of reducing r_{cont} to 50 $\mu\Omega cm^2$ on nominal efficiencies and electric powers.

percentage points or 5.8–6.8%, respectively, followed by those of the CTC in Fig. 2(b). The latter shows the same increases as the CTC in Fig. 2(c) only at $T_R = 563$ K.

3.7. Effect of temperature drop at cold junction of bottom unicouple

The present calculations assume a temperature difference, $\Delta T_{cj,R} = 25$ K between the cold junctions of the bottom unicouples of the CTCs in Figs. 2(a)–(c) and the heat rejection radiator. However, actual values could be lower or higher than 25 K, depending on the material selection and layering at the cold junctions, which would affect the performance of the CTCs. Since the design of the actual structure between the cold junctions of the bottom unicouples and heat rejection radiator is outside the scope of the present analysis, calculations are performed to quantify the effect of changing $\Delta T_{cj,R} = (T_{c,B} - T_R)$ on the performance of the CTCs. Fig. 12 plots the ratios of the nominal peak efficiencies of the CTCs, η_{CTC}, and those calculated earlier at $\Delta T_{cj,R} = 25$ K, $\eta_{CTC@\Delta T_{jc,R}}$. As this figure indicates, the relative nominal efficiencies of the CTCs changes linearly with $\Delta T_{cj,R}$. The efficiencies at $\Delta T_{jc,R} = 0.0$ K, which represent the theoretical values for the CTCs, increase by ~2.15–6.5%, depending on the value of T_R and the configuration of the CTC. The increases in the nominal peak efficiencies of the CTCs are larger the higher is T_R, and the highest is for the CTC in Fig. 2(a), followed by those for the CTCs in Figs. 2(b) and (c), respectively. Conversely, the conversion efficiencies of the CTCs decrease as $\Delta T_{cj,R}$ increase beyond 25

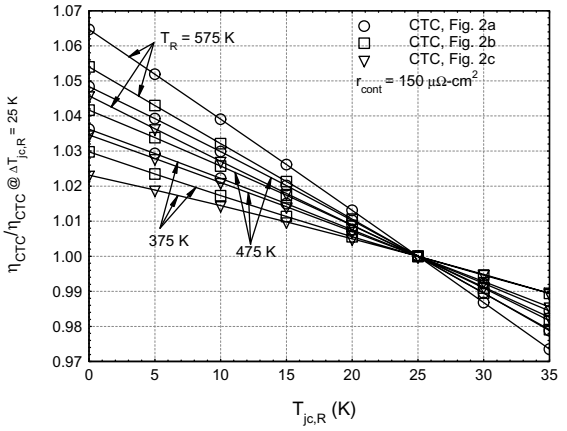

Fig. 12. Effect of $\Delta T_{cj,R}$ on nominal efficiencies.

K. The results in Fig. 12 indicate that increasing $\Delta T_{cj,R}$ from 25 to 35 K decreases the nominal peak efficiencies of the CTCs by ~1.0–2.8%.

3.8. Cross-sections areas of optimized n- and p-legs

An important design consideration that affects the integration of the top and bottom unicouples in the CTCs is the ratio of the cross-section areas of the n- and p-legs of the top SiGe unicouple, $(A_n + A_p)_T$, and of the bottom unicouples, $(A_n + A_p)_B$, Γ:

$$\Gamma = \lfloor A_n + A_p \rfloor_T / \lfloor A_n + A_p \rfloor_B \quad (2)$$

This ratio is shown in Fig. 13 to be independent of the input thermal power, $Q_{in,CTC}$ but increases as the heat rejection temperature, T_R, decreases. It is worth noting that the cross-section areas of the n- and p-legs of the top SiGe unicouples are independent of T_R but increase linearly with $Q_{in,CTC}$, while those of the bottom unicouples increase linearly with either $Q_{in,CTC}$ or T_R

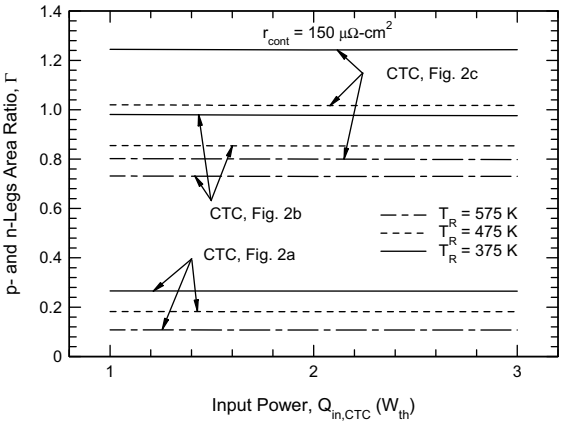

Fig. 13. Ratio of optimized n- and p-legs of top and bottom unicouples.

(Table 1). For the n- and p-legs of the top SiGe unicouple in Fig. 2(a), when $T_{c,T}$ = 780 K, the average input heat flux = 29.0 W_{th}/cm^2, the electrical power density = 1.70 W_e/cm^3 and the specific power = 569 W_e/kg. Because the cold junction temperature, $T_{c,T}$, for the SiGe unicouple in Figs. 2(b) and (c) is higher (980 K), the average input heat flux, electrical power density and specific power for the n-and p-legs are lower; 17.6 W_{th}/cm^2, 0.60 and 202 W_e/kg, respectively (Table 1).

As indicated in Fig. 13, the area ratios, Γ, for the CTC in Fig. 2(c) are the highest, followed by those for the CTC in Fig. 2(b), then those for the CTC in Fig. 2(a). For the CTC in Fig. 2(c), these area ratios are 1.24, 1.02 and 0.8 when T_R = 375, 475 and 575 K, respectively (Fig. 13). The corresponding values for the CTC in Fig. 2(b) are 0.98, 0.85 and 0.73 and only 0.27, 0.18 and 0.11, respectively, for the CTC in Fig. 2(a). The indicated increases in Γ with decreasing T_R, are indicative of the decreases in the areas of the optimized n- and p-legs of the bottom unicouples, and since the densities of the thermoelectric materials of the bottom unicouples of the CTCs in Figs. 2(a)–(c) are more than twice that of SiGe (ρ_{SiGe} = 2.99 g/cm^3, $\rho_{2N-PbTe}$ = 8.242 g/cm^3, $\rho_{TAGS-85}$ = 6.313 g/cm^3, $\rho_{CeFeCoSb}$ = 7.85 g/cm^3, ρ_{CoSb} = 7.62 g/cm^3, and ρ_{ZnSb} = 6.542 g/cm^3), decreasing T_R increases the electric power density and the specific power of the CTCs (Table 1).

4. Discussion and applications

Results of the present analyses show that CTCs are a viable and very promising energy conversion option for ARPSs compared to SOA SiGe [17]. The top SiGe unicouples in the CTCs investigated have an excellent track record on numerous missions that employed RTGs successfully for more than two decades [1–3]. The nominal conversion efficiency of the CTC with a bottom unicouple that is made of off-the-shelf thermoelectric materials (p-leg TAGS-85 and n-leg 2N–PbTe) is 14.1%, 11.9% and 9.4% when the heat rejection temperature, T_R = 375, 475 and 575 K, respectively. These materials have well known properties and fabrication and handling techniques and have been flown on space missions successfully but less than SiGe.

Assuming a thermal efficiency of 90% and electric losses of 5% for the ARPSs, their conversion efficiencies would be 12.72%, 10.73% and 8.48% when T_R = 375, 475 and 575 K, respectively (Table 2). These efficiencies are 110%, 80% and 40% higher than that of the SOA RTGs, when operated at the same hot junction temperature of 1273 K and a cold junction temperature of 575 K, resulting in similar percentage decreases in the amount of $^{238}PuO_2$ fuel needed for same electrical power level. Despite the high density of the TAGS-85 and 2N–PbTe compared to that of the SiGe, the savings in the $^{238}PuO_2$ fuel mass and number of GPHS bricks for the ARPS would more than compensate for the higher mass of these thermoelectric materials in the bottom unicouple of the CTC in Fig. 2(a), resulting in higher specific power for the ARPS compared to SOA RTG [17].

The two CTCs in Figs. 2(b) and (c) employ segmented and Skuterudites bottom unicouples, respectively. The materials of these unicouples have high FOM in the temperature range from 450 to 973 K (Fig. 1). The Skuterudites have demonstrated performance at high efficiency up to 13.8% in recent laboratory tests performed both at JPL and UNM-ISNPS at hot and cold junction temperatures of 973 and 300 K, respectively. The Skutterudites device technology is currently at TRL-3 and could be advanced to TRL-5 within the next 2–3 years. Skutterudites are heavier than SiGe, but the high efficiency and the resulting reduction in the mass of the $^{238}PuO_2$ fuel more than compensate for the high Skutterudites density ($\rho_{CeFeCoSb}$ = 7.85 g/cm^3, ρ_{CoSb} = 7.62 g/cm^3),

resulting in a lower total mass and much higher specific power for the ARPS, compared to SOA RTGs [17]. Present results indicate that the CTC with segmented bottom unicouple (Fig. 2(b)) is the most promising with a device peak efficiency of 14.32% when T_R = 375 K; this efficiency decreases to 10.13% when T_R increases to 575 K. With the same thermal efficiency and electrical losses indicated earlier, the conversion efficiency of the ARPS with the CTC in Fig. 2(b) would be 12.923% and 9.14% when T_R = 375 and 575 K, respectively, once again significantly higher than that for SOA RTG at same hot junction temperature of 1273 K and cold junction temperature of 566 K (~4.6%).

The calculated nominal peak efficiencies of the CTCs analyzed in this paper assuming a contact resistance of 150 $\mu\Omega cm^2$ per leg in the top and bottom unicouples are conservative. When this contact resistance per leg decreases to a more realistic value of 50 $\mu\Omega cm^2$, the nominal peak efficiencies of the CTCs increase by 0.3–0.9 percentage points, depending on the value of T_R and the materials of the bottom unicouples (Figs. 2 and 11).

In summary, CTCs are a viable option and should be developed and considered for future use in ARPSs. These ARPSs could be modular for meeting various electric powers for a spectrum of interplanetary missions from 20.0 to 1.0 kW_e. The resulting saving in the mass of the $^{238}PuO_2$ fuel and the high specific power for these ARPSs would effectively reduce the mission cost. At a radiator temperature of 575 K, the CTCs investigated in this paper could also be considered for use in space nuclear reactor power systems at electrical powers of 10–50 kW_e, without requiring very large radiators. For higher electrical power levels, however, a higher radiator temperature of 680–750 K would be needed for manageable heat rejection radiator area and attractive system specific power ($\geqslant$ 20 W_e/kg). At these radiator temperatures, the CTCs investigated in this paper might still be more efficient than SOA SiGe, resulting in a lower system alpha, which could be the subject of a future investigation.

5. Summary and conclusions

The performance of three CTCs is investigated for potential use in ARPSs having electric power requirements ranging from 20.0 to 1.0 kW_e to enable a number of future space exploration missions. The CTCs have significantly higher conversion efficiencies than SiGe convertors used in SOA RTG. Each is comprised of a SiGe top unicouple that is thermally, but not electrically, coupled to a bottom unicouple with one of the following thermoelectric materials: (a) p-leg of TAGS-85 and n-leg of 2N–PbTe; (b) p-leg of $CeFe_{3.5}Co_{0.5}Sb_{12}$ and n-leg of $CoSb_3$; and (c) segmented p-leg of $CeFe_{3.5}Co_{0.5}Sb_{12}$ and Zn_4Sb_3 and n-leg of $CoSb_3$. The analyses are performed at constant hot shoe temperature = 1273 K for the top SiGe unicouples, which is the same as that of the SiGe unicouples in SOA RTG, but the values of the cold junction temperature depend on the thermoelectric materials for the bottom unicouple (780 K for the CTC in Fig. 2(a) and 980 K for the CTCs in Figs. 2(b) and (c)).

The cross section areas of the n- and p-legs in the top SiGe unicouples are first optimized at the nominal hot and cold junction temperatures and thermal power input of 1.0, 2.0 or 3.0 W_{th}. Then, the dimensions of the n- and p-legs of the bottom unicouples in the CTCs are optimized for maximum efficiency operation, subject to the following constraints: (a) constant hot junction temperatures that are 20 K lower than the cold junction temperature of the top SiGe unicouples; (b) the

thermal power input is the same as the rejection thermal power from the top SiGe unicouple; (c) nominal cold junction temperatures of 400, 500, or 600 K. The heat rejection temperatures are taken 25 K lower than the cold junction temperatures of the bottom unicouples. For the CTCs, the lengths of the top and bottom unicouples are equal (10 mm) and the nominal operation parameters (conversion efficiency and electrical power) are those corresponding to the peak conversion efficiency of the top SiGe unicouples.

When assuming a thermal efficiency of 90% and electric losses of 5% for an ARPS with CTCs, its conversion efficiecy could be 40–110% higher than that of SOA RTG, depending on the value of the heat rejection temperature. Such high ARPS's efficiencies would significantly reduce the amount of $^{238}PuO_2$ fuel, the total system mass and the mission cost. The calculated nominal conversion efficiencies and electrical powers of the CTCs with a contact resistance of 150 $\mu\Omega cm^2$ per leg in the top and bottom unicouples are conservative. Decreasing this resistance to a more realistic 50 $\mu\Omega cm^2$ increases the estimates for the ARPS nominal efficiency and electrical power by ~0.3–0.9 percentage points, depending on the thermoelectric materials of the bottom unicouples and the heat rejection temperature. At the high radiator temperature of 575 K, the CTCs could be used in space nuclear reactor power systems for electrical powers of 10–30 kW_e to enable future planetary surface missions without requiring a very large radiator. For higher electrical power levels, however, higher radiator temperatures of 650 to 750 K would be needed for a manageable radiator area and attractive system specific power and total mass and size.

The SiGe used in the top unicouples of the three CTCs analyzed in this paper has an excellent track record on many missions that employed RTGs. One of the CTCs developed and investigated in this paper uses a bottom unicouple having a p-leg of TAGS-85 and an n-leg of 2N–PbTe (Fig. 2(a)). These thermoelectric materials have well known properties and fabrication and handling techniques and space flight experiences, but less than SiGe. The other two CTCs in Figs. 2(b) and (c) employ segmented and Skutterudites bottom unicouples. Skutterudites have high FOMs in the temperature range from ~450 to 973 K and demonstrated efficiency of ~13.8% at hot and cold junction temperatures of 973 and 300 K, however the device technology is currently at TRL-3 and could be advanced to TRL-5 within the next 2–3 years. These materials and both TAGS-85 and 2N–PbTe used in the bottom unicouples of the CTCs in Fig. 2 are heavier than SiGe, but the high efficiencies of the CTCs more than compensate for the high densities of these materials, resulting in higher specific power ARPSs and much less $^{238}PuO_2$ fuel than SOA RTGs.

Acknowledgements

This work is funded under NASA grant no. NAG3-2543 to the University of New Mexico's Institute for Space and Nuclear Power Studies. The opinions expressed in this article are solely those of the authors and have neither been endorsed by nor reflect an official position of NASA.

References

[1] Bennett G, Lombardo J, Rick B. Power performance of the general-purpose heat source radioisotope thermoelectric generator. In: El-Genk MS, Hoover M, editors. Proc space nuclear power and propulsion. Space nuclear power systems, vol. 5.

[2] Carpenter RT. Status of US radioisotope space power system. Isot Radiat Technol 1970;9(3):330–44.
[3] Fiehler D, Oleson S. Mission steering profiles of outer planetary orbiters using radioisotope electric propulsion. In: El-Genk MS, editor. Proc of space technology and applications int forum, AIP proceedings no 669. Melville, NY: American Institute of Physics; 2004. p. 248–55.
[4] Marriort A, Fujita T. Evolution of SP-100 system designs. In: El-Genk MS, Hoover MD, editors. Proceedings of space nuclear power and propulsion no 301. New York, NY: American Institute of Physics; 1994. p. 157–69.
[5] El-Genk MS, Seo JT. SNPSAM-space nuclear power system analysis model. In: El-Genk MS, Hoover MD, editors. Space nuclear power systems 1986, CONF-860102, vol. 5. Malabar, FL: Orbit Book Company; 1987. p. 111–23.
[6] Angelo Jr JA, Buden D. Space nuclear power. Malabar, FL: Orbit Book Company; 1985. p. 133–7.
[7] Caillat T, Borshchevsky A, Snyder J, Fleurial J-P. High efficiency segmented thermoelectric unicouples. In: El-Genk MS, editor. Proc of space technology and applications int forum (STAIF-00), AIP conference proceedings no 504. Melville, NY: American Institute of Physics; 2000. p. 1508–12.
[8] El-Genk MS, Saber HH, Caillat T. Efficient, segmented thermoelectric for space power applications. J Energy Convers Manage 2003;44(11):1755–72.
[9] El-Genk MS, Saber HH. High efficiency segmented thermoelectric for operation between 973 K and 300 K. Energy Convers Manage 2003;44(7):1069–88.
[10] El-Genk MS, Saber HH. Predictions of segmented thermoelectric unicouples performance at hot temperatures $\leqslant 873$ K and cold temperature of 298 K. In: Proc of 21st int conf on thermoelectrics. Piscataway, NJ: IEEE; 2002. p. 408–11.
[11] El-Genk MS, Saber HH. Performance optimization of segmented thermoelectric unicouples. In: El-Genk MS, editor. Proc of space technology and applications int forum (STAIF-02), AIP conference proceedings no 608. NY: American Institute of Physics; 2002. p. 980–8.
[12] El-Genk MS, Saber HH, Sakamoto J, Caillat T. Life tests of Skutterudite thermoelectric unicouple (MAR-03). In: Proceedings of 22nd international conference of thermoelectrics (ICT-2003). Piscataway, NJ: IEEE; 2003. p. 417–20.
[13] El-Genk MS, Saber HH, Caillat T. Performance tests of Skutterudites and segmented thermoelectric converters. In: El-Genk MS, editor. Proc of space technology and applications int forum (STAIF-04), AIP conference proceedings no 669. Melville, NY: American Institute of Physics; 2004. p. 541–52.
[14] El-Genk MS. Energy conversion technologies for advanced radioisotope and nuclear reactor power systems for future exploration. In: Proc 21st int conf on thermoelectrics. Piscataway, NJ: IEEE; 2002. p. 375–80.
[15] Fleurial J-P, Borshchevsky A, Caillat T, Morelli D, Meisner G. High figure of merit in Ce-filled Skutterudites, In: Proc of 15th international conference on thermoelectric, IEEE catalog 96TH8169; 1996, p. 91.
[16] Fleurial J-P, Borshchevsky A, Caillat T, Ewell R. New materials and devices for thermoelectric applications. In: Proceedings of 32th Intersociety Energy Conversion Engineering Conference, vol. 2; 1997, p. 1080.
[17] El-Genk MS, Saber HH. Cascaded thermoelectric conversion-advanced radioisotope power systems (CTC-ARPSs). In: El-Genk MS, editor. Proc of space technology and applications int forum (STAIF-04), AIP conference proceedings no 669. Melville, NY: American Institute of Physics; 2004. p. 230–41.